hv photonics

IMPACT FACTOR 2.1

CITESCORE 2.6

Review

Angular Deviations, Lateral Displacements, and Transversal Symmetry Breaking: An Analytical Tutorial

Stefano De Leo and Marco Mazzeo

Special Issue

Structured Light Beams: Science and Applications

Edited by

Dr. A. Srinivasa Rao and Dr. Andra Naresh Kumar Reddy

MDPI

https://doi.org/10.3390/photonics11060573

photonics

MDPI

Review

Angular Deviations, Lateral Displacements, and Transversal Symmetry Breaking: An Analytical Tutorial

Stefano De Leo [1,*,†] and Marco Mazzeo [2,†]

[1] Department of Applied Mathematics, State University of Campinas, Campinas 13083-859, Brazil
[2] Department of Mathematics and Physics, Salento University, 73100 Lecce, Italy; marco.mazzeo@unisalento.it
* Correspondence: deleo@unicamp.br
† These authors contributed equally to this work.

Abstract: The study of a Gaussian laser beam interacting with an optical prism, both through reflection and transmission, provides a technical tool to examine deviations from the optical path as dictated by geometric optics principles. These deviations encompass alterations in the reflection and refraction angles, as predicted by the reflection and Snell laws, along with lateral displacements in the case of total internal reflection. The analysis of the angular distributions of both the reflected and transmitted beams allows us to understand the underlying causes of these deviations and displacements, and it aids in formulating analytic expressions that are capable of characterizing these optical phenomena. The study also extends to the examination of transverse symmetry breaking, which is a phenomenon observed in the laser beam as it traverses the oblique interface of the prism. It is essential to underscore that this analytical overview does not strive to function as an exhaustive literature review of these optical phenomena. Instead, its primary objective is to provide a comprehensive and self-referential treatment, as well as give universal analytical formulas intended to facilitate experimental validations or applications in various technological contexts.

Keywords: Goos–Hänchen shift; angular deviations; transversal symmetry breaking

Citation: De Leo, S.; Mazzeo, M. Angular Deviations, Lateral Displacements, and Transversal Symmetry Breaking: An Analytical Tutorial. *Photonics* **2024**, *11*, 573. https://doi.org/10.3390/photonics11060573

Received: 9 May 2024
Revised: 15 June 2024
Accepted: 17 June 2024
Published: 19 June 2024

1. Introduction

Gaussian optical beams, characterized by their distinctive intensity profile that follows a bell-shaped curve across their cross-section, play a fundamental role in the field of optics [1,2]. They serve as a cornerstone in various sectors, with versatile applications spanning from laser technology [3] to telecommunications [4], as well as astronomy [5] and medical imaging [6]. A comprehensive understanding of Gaussian optical beams is crucial for designing optical systems and harnessing light for a wide range of practical and diversified purposes. Studying the propagation of Gaussian lasers through an optical prism enables the comprehension of optical phenomena, such as angular deviations [7–10] from the reflection and Snell laws, lateral shifts [11–15] known as Goos–Hänchen shifts—named in honor of the German physicists who first reported experimental evidence in 1947 [16–18]—and, last but not least, the phenomenon of transverse symmetry breaking. An additional advantage lies in the swift and cost-effective realization of experiments confirming these optical phenomena [19–21].

It is worth noting that due to the mathematical similarity between the Helmholtz equation in the paraxial limit [1,2] and the Schrödinger equation [22], the typical phenomena of nonrelativistic quantum mechanics such as delay times and resonant tunneling can be readily simulated in an optics laboratory [23–25].

The primary objective of this tutorial is to provide a comprehensive mathematical analysis of the behavior of Gaussian beams when incident on an isotropic prism and to offer a detailed and rigorous treatment that could serve as a foundational reference for further studies in this area. The mathematical insights and general formulas derived can

be instrumental for researchers working on related optical systems and applications. This theoretical groundwork could be useful for advancing practical implementations and for developing new optical devices.

Three optical phenomena of great interest, both from a theoretical and an experimental perspective, will be analyzed in detail in this tutorial: the angular deviation of a laser beam reflected or transmitted by an optical prism compared to the optical path predicted by the reflection and Snell laws, the lateral shift in the case of total internal reflection, and finally, the breaking of transverse symmetry. The analytical description that will enable the understanding of these phenomena is based on the integral representation of the incident optical beam and, consequently, of the reflected and transmitted beams. The technical details will be covered in the next section. However, to facilitate an understanding for readers unfamiliar with these aspects, we will briefly and qualitatively discuss what causes these phenomena. As mentioned earlier, in the upcoming sections, we will analyze these phenomena in detail using an appropriate analytical representation of the beams, thus addressing them from both a qualitative and quantitative perspective.

The angular distribution of a Gaussian laser beam incident on a dielectric block, as shown in Figure 1, is a symmetric distribution centered around the angle α in the x–z plane (the plane of Figure 1) and at the angle 0 in the y–z plane (where y is the axis perpendicular to the plane of incidence shown in Figure 1). Thus, the optical beam will move while maintaining its maximum intensity along the z axis. For the reflected and transmitted fields, the Fresnel coefficients are real and modulate the angular distribution of the incident beam. This modulation causes a breaking of angular symmetry, thus resulting in a deviation from the optical path predicted by the reflection and Snell laws. This breaking of angular symmetry should not be confused with the breaking of transverse symmetry. For example, the reflected field will exhibit angular deviations from the optical path predicted by the law of reflection, but it will maintain its transverse symmetry in the coordinates perpendicular to the axial direction. The same applies to the field transmitted through the lateral interface due to the equality of the angles of incidence and transmission. Transverse symmetry is, however, broken for the beam transmitted at an angle different from the incidence angle by the oblique surface. We will refer to this phenomenon as the breaking of transverse symmetry to distinguish it from the breaking of angular symmetry that causes angular deviations. The final phenomenon, but certainly not the least important, is the lateral shift, also known as the Goos–Hänchen effect. This phenomenon occurs when the Fresnel coefficient has a phase, as is the case with total internal reflection. This phase affects not the angular distribution but the spatial components of the plane wave solution of the paraxial Helmholtz equation.

The tutorial is structured as follows. In the next section, as previously mentioned, we will introduce the integral form of the incident field, the reflected field, and the fields transmitted through the oblique and lateral interfaces. This will establish the notation and identify the terms responsible for the optical phenomena under study. In Section 3, we will compute the Fresnel coefficients in the case where the dielectric axial discontinuity is not fixed at zero, as is typically assumed in textbooks [1,2]. Indeed, in the case of a prism, it is evident that choosing to set the dielectric discontinuity of the upper interface to $\widetilde{z} = 0$, see Figure 2, which experimentally means fixing at the upper interface the minimum belt of the incoming beam, implies that the dielectric discontinuities of the oblique and lateral interfaces will be located respectively at $z_* = d/\sqrt{2}$ and $\widetilde{x} = l - d$, as shown in Figures 1 and 2. In the same section, we will compute the first-order series expansion of the Fresnel coefficients, which will later prove useful for integrating the reflected and transmitted fields. In Section 4, we will explore the intricacies of optical phase analysis. This examination will empower us to deduce the optical path of a beam, as predicted by geometric optics through a straightforward derivative. Furthermore, it will illuminate the reasons behind the transverse symmetry breakdown observed in the case of a beam transmitted through the oblique interface. Within this section, we will present the streamlined integral expressions for both reflected and transmitted fields. This will pave the way

for straightforward integrations in the subsequent section, thereby allowing us to derive closed-form formulas for optical beams reflected by and transmitted through the prism. Section 5 will cover optical phenomena, including angular deviation, lateral displacement, and transverse symmetry breaking for beams reflected and transmitted through the optical prism. We aim to derive analytical formulas wherever possible, which are beneficial for experiment preparation and potentially applicable in technological developments. Final considerations will be presented in the concluding section, where we will briefly introduce the weak measurement technique [26], which is a highly useful amplification technique for the experimental verification of angular deviations and lateral displacements.

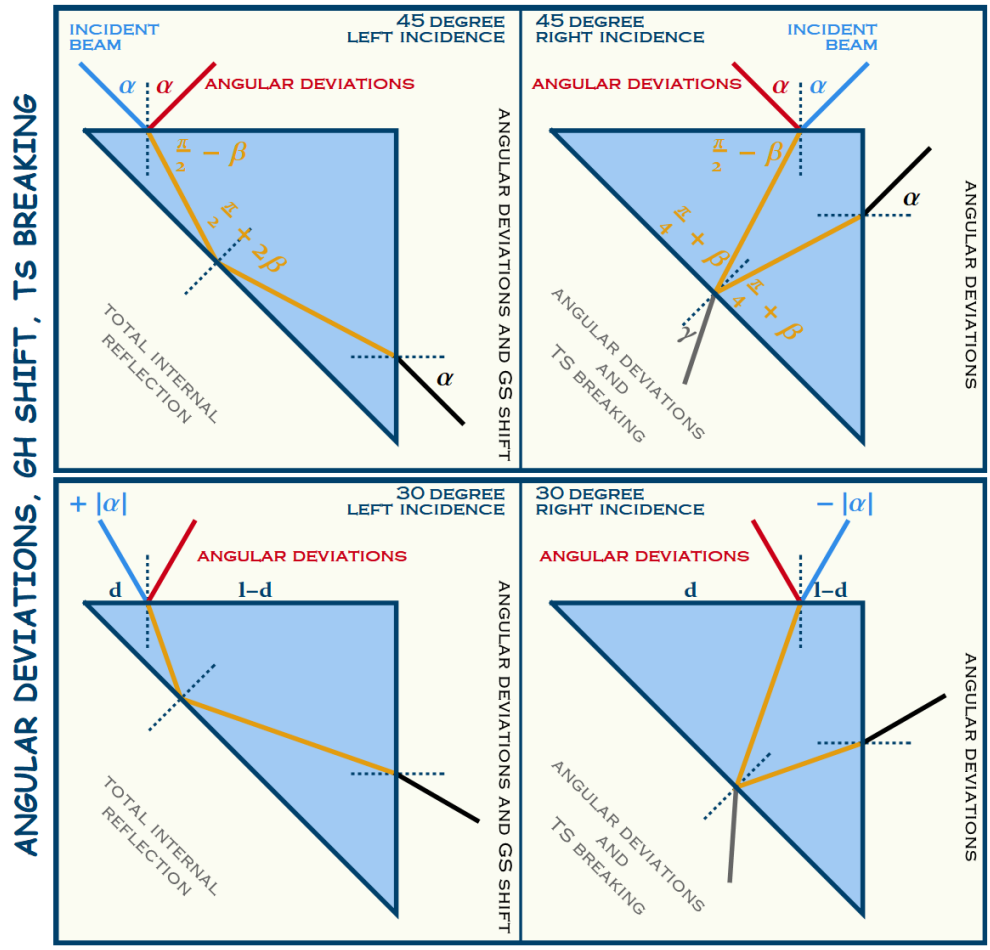

Figure 1. The incident optical beam impacts the upper face of the prism at an angle α (blue line) and is partially reflected at the same angle of incidence (red line) while also partially transmitted at an angle β (orange line). During its propagation inside the prism, the optical beam is partly or entirely reflected from the oblique surface (angled at 45° to the upper interface). The prism geometry determines a reflection angle on the oblique interface of $\frac{\pi}{4} + \beta$ in the case of left-side incidence and $\frac{\pi}{4} - \beta$ in the case of right-side incidence, so we can consider positive angles for left-side incidence and negative angles for right-side incidence. Upon striking the lateral face at an angle β, it is then transmitted into the air at an angle α (black line). The optical beams depicted in the figure replicate the real situation for a BK7 prism with a refractive index 1.515 for a 638 nm red laser. In this case, total internal reflection occurs for incidence angles greater than $-5.603°$.

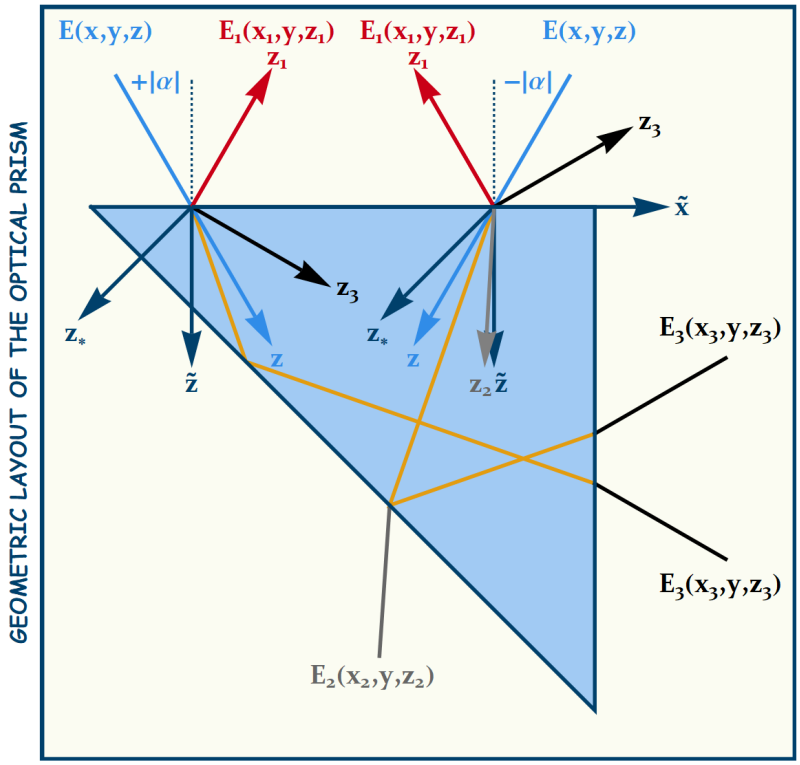

Figure 2. The figure shows the coordinate axes of each of the three interfaces: $(\tilde{x}, \tilde{z})$ for the upper interface, (x_*, z_*) for the oblique face, and $(\tilde{z}, \tilde{x})$ for the lateral face. The second coordinate of the axes represents the axis perpendicular to each of the interfaces. The coordinate axes of the incident beam, the beam reflected from the upper interface, the beam reflected from the oblique interface, and the beam transmitted from the lateral interface are respectively represented by (x, z), (x_1, z_1), (x_2, z_2), and (x_3, z_3). The second coordinate of the axes denotes the axial path of the optical beams as predicted by the laws of geometric optics: z for the incident beam, z_1 for the reflected beam, z_2 for the beam transmitted through the oblique interface, and z_3 for the beam transmitted through the lateral interface.

2. The Integral Form of the Optical Beams

In the case of an optical beam propagating along the z direction, the irradiance is given by

$$I(x,y,z) \;=\; I_0 \left[\frac{\mathrm{w}_0}{\mathrm{w}(z)}\right]^2 \exp\left[-2\,\frac{x^2+y^2}{\mathrm{w}^2(z)}\right], \tag{1}$$

where $I_0 = 2\,P\,/\,\pi\,\mathrm{w}_0^2$, P is the total power, there is the same across all beam cross-sections, w_0 denotes the beam waist radius, and $\mathrm{w}(z) = \mathrm{w}_0\sqrt{1+(z/z_\mathrm{R})^2}$, where $z_\mathrm{R} = \pi\,\mathrm{w}_0^2\,/\,\lambda$ is the Raleigh range (defined as the distance over which the beam radius spreads by a factor of $\sqrt{2}$), and λ represents the wavelength [1–3].

Revisiting how we obtain the previous expression starting from the angular distribution of the electric field is crucial in understanding how Fresnel coefficients, by modifying the angular distribution and/or the optical phase of the beam, generate deviations from the laws of geometric optics, such as angular deviations and lateral displacements. The electric field of the optical beam propagating from the laser source to the first interface of an optical prism, see Figure 1, can be expressed as a superposition of plane wave solutions of Maxwell's equations:

$$\begin{aligned}\exp[\,i\,(k_{\tilde{x}}\,\tilde{x} + k_y\,y + k_{\tilde{z}}\,\tilde{z})\,] \;&=\; \exp[\,i\,k\,[\,(\,\tilde{x}\,\sin\alpha_x + \tilde{z}\,\cos\alpha_x\,)\,\cos\alpha_y + y\,\sin\alpha_y\,]\,]\\ &=\; \exp[\,i\,\psi(\alpha_x,\alpha_y)\,]\,,\end{aligned} \tag{2}$$

as follows

$$E(x,y,z) \;=\; E_0 \int \mathrm{d}\alpha_x \,\mathrm{d}\alpha_y \; g(\alpha_x,\alpha_y) \;\exp\left[\, i\,\psi(\alpha_x,\alpha_y)\,\right] , \tag{3}$$

where, for a Gaussian laser, the angular distribution is given by

$$g(\alpha_x,\alpha_y) \;=\; \frac{z_{\mathrm{R}}}{\lambda}\,\exp\left\{-\left(\frac{z_{\mathrm{R}}}{\mathrm{w}_0}\right)^2\left[\,(\alpha_x-\alpha)^2+\alpha_y^2\,\right]\right\} , \tag{4}$$

and α is the angle of incidence in the $(\tilde{x},\tilde{z})$ plane, $\tilde{z}$ is the axis perpendicular to the first interface—see Figure 2—and $k = 2\,\pi/\,\lambda$.

The condition $\mathrm{w}_0 \gg \lambda$, which is easily achievable, for instance, with red ($\lambda = 638$ nm) or green ($\lambda = 532$ nm) laser beams, entails sharply peaked angular distributions. Consequently, instead of the optical phase given in (2), we can employ its Taylor expansion up to the second order around the angle $(\alpha_x,\alpha_y) = (\alpha,0)$,

$$\begin{aligned}\psi(\alpha_x,\alpha_y)\,/\,k \;\approx\;& \tilde{x}\,\sin\alpha \,+\, \tilde{z}\,\cos\alpha \,+\, (\,\tilde{x}\,\cos\alpha \,-\, \tilde{z}\,\sin\alpha\,)\,(\,\alpha_x \,-\, \alpha\,) \,+\, y\,\alpha_y \\ & -\,(\,\tilde{x}\,\sin\alpha \,+\, \tilde{z}\,\cos\alpha\,)\,\frac{(\,\alpha_x \,-\, \alpha\,)^2 \,+\, \alpha_y^2}{2}\;.\end{aligned} \tag{5}$$

The previous phase can be reformulated by utilizing the intrinsic coordinates of the optical beam, which are denoted as (x,z). We o bserve that these axes can be obtained through a rotation of the proper axes of the first interface $(\tilde{x},\tilde{z})$; see Figure 2:

$$\begin{pmatrix} x \\ z \end{pmatrix} \;=\; \begin{pmatrix} \cos\alpha & -\sin\alpha \\ \sin\alpha & \cos\alpha \end{pmatrix}\begin{pmatrix} \tilde{x} \\ \tilde{z} \end{pmatrix} , \tag{6}$$

where we obtain

$$\psi(\alpha_x,\alpha_y)\,/\,k \;\approx\; z \,+\, x\,(\,\alpha_x \,-\, \alpha\,) \,+\, y\,\alpha_y \,-\, z\,\frac{(\,\alpha_x \,-\, \alpha\,)^2 \,+\, \alpha_y^2}{2}\;. \tag{7}$$

The electric field of the incident optical beam can thus be rewritten as follows:

$$E(x,y,z) \;=\; E_0\exp[\,i\,k\,z\,]\,A(x,y,z) \tag{8}$$

where

$$\begin{aligned}A(x,y,z) \;=\;& \int \mathrm{d}\alpha_x \;\mathrm{d}\alpha_y \; g(\alpha_x,\alpha_y) \;\times \\ & \exp\left\{\, i\,k\left[\, x\,(\,\alpha_x \,-\, \alpha\,) \,+\, y\,\alpha_y \,-\, z\,\frac{(\,\alpha_x \,-\, \alpha\,)^2 \,+\, \alpha_y^2}{2}\,\right]\right\} .\end{aligned} \tag{9}$$

It is straightforward to verify that $A(x,y,z)$ satisfies the Hemoltz equation within the paraxial limit:

$$\left(\frac{\partial^2}{\partial x^2} \,+\, \frac{\partial^2}{\partial y^2} \,+\, 2\,i\,k\,\frac{\partial}{\partial z}\right) A(x,y,z) \;=\; 0\;. \tag{10}$$

Additionally, the transverse symmetry in $A(x,y,z)$ is evident. In fact, through a simple change of the integration variables, we can rewrite the field $A(x,y,z)$ as follows:

$$A(x,y,z) \;=\; a(x,z)\,a(y,z) \tag{11}$$

where

$$a(r,z) = \frac{1}{\sqrt{\pi}} \int \mathrm{d}\rho \, \exp\left[-\rho^2 \left(1 + i \frac{z}{z_\mathrm{R}} \right) + 2\, i\, \rho \, \frac{r}{\mathrm{w}_0} \right] = \frac{\exp\left[- \dfrac{(\, r \,/\, \mathrm{w}_0 \,)^2}{1 + i\, z \,/\, z_\mathrm{R}} \right]}{\sqrt{1 + i\, z \,/\, z_\mathrm{R}}} \, . \tag{12}$$

The incident electric field is therefore described by the following expression:

$$E(x,y,z) = \frac{E_0 \, e^{i\, k\, z}}{1 + i\, z \,/\, z_\mathrm{R}} \, \exp\left[- \frac{(\, x^2 + y^2 \,) \,/\, \mathrm{w}_0^2}{1 + i\, z \,/\, z_\mathrm{R}} \right] \tag{13}$$

and the square modulus of this leads to Equation (1). Presenting the analytical characteristics of the incident optical beam allows us to introduce the reflected field and the fields transmitted by the prism using the same notation as employed for the incident beam. Without delving into technical details, such as solving intricate integrals (which will be addressed in the following sections), this approach helps us grasp which terms in the integrand functions will account for phenomena like angular deviations, lateral displacements, and the breakdown of transverse symmetry.

To represent the optical beams after interacting with the prism, we can employ the following electric fields:

$$E_s^{[\sigma]}(x_s, y, z_s) = E_0 \int \mathrm{d}\alpha_x \, \mathrm{d}\alpha_y \, g_s^{[\sigma]}(\alpha_x, \alpha_y) \, \exp\left[\, i\, \psi_s(\alpha_x, \alpha_y) \, \right] \tag{14}$$

where the subscript $s = 1$ refers to the beam reflected from the upper interface, the subscript $s = 2$ corresponds to the beam transmitted through the oblique interface (inclined at 45 degrees compared to the upper one), and the subscript $s = 3$ pertains to the beam that, after reflection from the oblique interface, is transmitted through the lateral interface (inclined at 90 degrees compared to the upper one). The upper index denotes the type of transverse wave: $\sigma =$ te for the transverse electric wave and $\sigma =$ tm for the transverse magnetic one.

The angular distribution of the beam reflected from the upper surface, $g_1^{[\sigma]}(\alpha_x, \alpha_y)$, is the product of the angular distribution of the incident beam, $g(\alpha_x, \alpha_y)$, with the Fresnel reflection coefficient, $f_1^{[\sigma]}(\alpha_x) = r_1^{[\sigma]}(\alpha_x)$. Since the Fresnel coefficient is real for both transverse electric and magnetic waves, it directly influences the incident angular distribution, thus causing a kind of angular symmetry break and resulting in a reflection angle that is different from what is predicted by geometric optics reflection law. Consequently, this phenomenon leads to deviations from the geometrical optical path, which increase with the growth of the axial distance of the reflected beam.

The beam transmitted through the first interface will then be reflected and, in the case of partial reflection, transmitted by the oblique interface. The angular distribution of the transmitted beam will be determined by the product of the angular distribution of the incident beam, $g(\alpha_x, \alpha_y)$, and the Fresnel coefficient $f_2^{[\sigma]}(\alpha_x) = t_1^{[\sigma]}(\alpha_x)\, t_2^{[\sigma]}(\alpha_x)$. In the case of partial internal reflection, $g_2^{[\sigma]}(\alpha_x, \alpha_y)$ will be real. Similar to the reflected beam, this will result in angular deviations from the optical path predicted by Snell's law. For the beam transmitted through the oblique interface, a new phenomenon known as transverse symmetry breaking will occur [27]. This is due to the fact that the angle of transmission at the oblique interface is different from the incidence one. In the series expansion of the optical phase, this difference leads to a factor that multiplies the transverse coordinate in the plane of the dielectric. Consequently, it creates an asymmetry with the transverse coordinate being perpendicular to the plane of the dielectric.

Finally, the beam transmitted through the lateral interface will be characterized by an angular distribution determined by the product of the incoming beam's angular distribution, $g(\alpha_x, \alpha_y)$, and the Fresnel coefficient $f_3^{[\sigma]}(\alpha_x) = t_1^{[\sigma]}(\alpha_x)\, r_2^{[\sigma]}(\alpha_x)\, t_3^{[\sigma]}(\alpha_x)$. In the case of total internal reflection, the coefficient $r_2^{[\sigma]}(\alpha_x)$ becomes complex, thereby inducing a lateral displacement in the beam known as the Goos–Hänchen shift [16]. This shift adds to the angular deviations caused by the coefficients $t_1^{[\sigma]}(\alpha_x)$ and $t_3^{[\sigma]}(\alpha_x)$. Since, in this scenario, the transmission angle from the lateral interface is equal to the angle of incidence—similar to the reflected beam—transverse symmetry is preserved.

3. The Fresnel Coefficients and Their Derivatives

In Figure 3, electric and magnetic fields for transverse waves are depicted: transverse electric waves on the left and magnetic on the right. As previously discussed in the preceding section, we will consider the scenario where the discontinuity occurs at a distance d from the coordinate origin, thus representing the point where our beam reaches its narrowest belt.

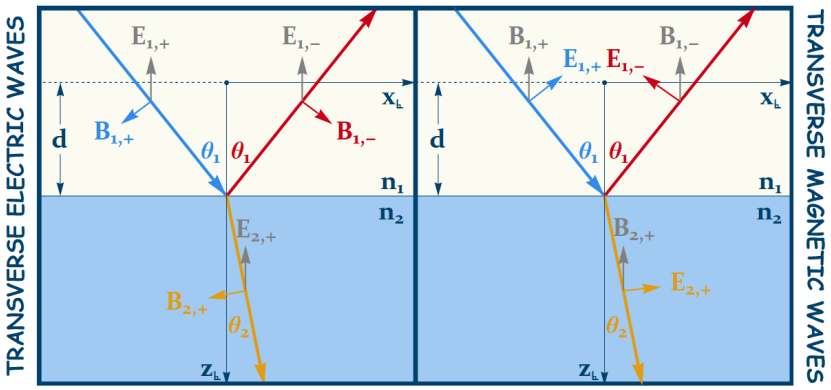

Figure 3. The figure illustrates the electric and magnetic fields of the incident, reflected, and transmitted waves for the case of waves with an electric field perpendicular to the plane of incidence (left side of the figure) and for the case of waves with a magnetic field perpendicular to the plane of incidence (right side of the figure). The interface between the two media is located at a distance d from the origin of the axes. This will allow us to calculate the Fresnel coefficients, which contain a phase responsible for the optical path of the beam.

By ensuring continuity between the electric and magnetic fields, we obtain

$$\begin{aligned} E_{1,+}^{[\mathrm{te}]}\, e^{i\, n_1 \cos\theta_1 kd} + E_{1,-}^{[\mathrm{te}]}\, e^{-i\, n_1 \cos\theta_1 kd} &= E_{2,+}^{[\mathrm{te}]}\, e^{i\, n_2 \cos\theta_2 kd}\,, \\ \cos\theta_1 \left(B_{1,+}^{[\mathrm{te}]}\, e^{i\, n_1 \cos\theta_1 kd} - B_{1,-}^{[\mathrm{te}]}\, e^{-i\, n_1 \cos\theta_1 kd} \right) &= \cos\theta_2\, B_{2,+}^{[\mathrm{te}]}\, e^{i\, n_2 \cos\theta_2 kd}\,, \end{aligned} \tag{15}$$

for transverse electric waves and

$$\begin{aligned} B_{1,+}^{[\mathrm{tm}]}\, e^{i\, n_1 \cos\theta_1 kd} + B_{1,-}^{[\mathrm{tm}]}\, e^{-i\, n_1 k \cos\theta_1 kd} &= B_{2,+}^{[\mathrm{tm}]}\, e^{i\, n_2 \cos\theta_2 kd}\,, \\ \cos\theta_1 \left(E_{1,+}^{[\mathrm{tm}]}\, e^{i\, n_1 \cos\theta_1 kd} - E_{1,-}^{[\mathrm{tm}]}\, e^{-i\, n_1 \cos\theta_1 kd} \right) &= \cos\theta_2\, E_{2,+}^{[\mathrm{tm}]}\, e^{i\, n_2 \cos\theta_2 kd}\,, \end{aligned} \tag{16}$$

for transverse magnetic waves. Rewriting the magnetic field in terms of the electric field and introducing the reflection $R^{[\sigma]} = E_{1,-}^{[\sigma]} / E_{1,+}^{[\sigma]}$ and transmission $T^{[\sigma]} = E_{2,+}^{[\sigma]} / E_{1,+}^{[\sigma]}$ coefficients Equations (15) and (16) reduce to

$$\begin{aligned} 1 + R^{[\mathrm{te}]}\, e^{-2\, i\, n_1 \cos\theta_1 kd} &= T^{[\mathrm{te}]}\, e^{i\, (\, n_2 \cos\theta_2 - n_1 \cos\theta_1\,)\, kd}\,, \\ 1 - R^{[\mathrm{te}]}\, e^{-2\, i\, n_1 \cos\theta_1 kd} &= \frac{n_2 \cos\theta_2}{n_1 \cos\theta_1}\, T^{[\mathrm{te}]}\, e^{i\, (\, n_2 \cos\theta_2 - n_1 \cos\theta_1\,)\, kd}\,, \end{aligned} \tag{17}$$

and

$$\begin{aligned} 1 + R^{[\mathrm{tm}]}\, e^{-2\,i\,n_1\cos\theta_1 kd} &= \frac{n_2}{n_1}\, T^{[\mathrm{tm}]}\, e^{i\,(\,n_2\cos\theta_2 - n_1\cos\theta_1\,)\,kd}\,, \\ 1 - R^{[\mathrm{tm}]}\, e^{-2\,i\,n_1\cos\theta_1 kd} &= \frac{\cos\theta_2}{\cos\theta_1}\, T^{[\mathrm{tm}]}\, e^{i\,(\,n_2\cos\theta_2 - n_1\cos\theta_1\,)\,kd}\,. \end{aligned} \tag{18}$$

Finally,

$$R^{[\sigma]} = r^{[\sigma]}\, e^{2\,i\,n_1\cos\theta_1 kd} \qquad \text{and} \qquad T^{[\sigma]} = t^{[\sigma]}\, e^{i\,(\,n_1\cos\theta_1 - n_2\cos\theta_2\,)\,kd}\,, \tag{19}$$

where

$$\{\, r^{[\mathrm{te}]}\,,\, t^{[\mathrm{te}]}\,\} = \left\{ \frac{n_1\cos\theta_1 - n_2\cos\theta_2}{n_1\cos\theta_1 + n_2\cos\theta_2}\,,\, \frac{2\,n_1\cos\theta_1}{n_1\cos\theta_1 + n_2\cos\theta_2} \right\}, \tag{20}$$

and

$$\{\, r^{[\mathrm{tm}]}\,,\, t^{[\mathrm{tm}]}\,\} = \left\{ \frac{n_2\cos\theta_1 - n_1\cos\theta_2}{n_2\cos\theta_1 + n_1\cos\theta_2}\,,\, \frac{2\,n_1\cos\theta_1}{n_2\cos\theta_1 + n_1\cos\theta_2} \right\}, \tag{21}$$

are the well-known Fresnel coefficients at the zero discontinuity [1,2].

As mentioned in the Introduction, in order to derive analytical formulas for optical beams reflected by and transmitted through the prism, we will expand the Fresnel coefficients in a Taylor series. It is therefore beneficial to obtain the derivatives of the Fresnel coefficients in their most general form, thereby allowing us to subsequently apply these formulas in the context of reflection by and transmission through the prism.

By deriving the reflection coefficients for transverse electric and magnetic waves and performing some algebraic manipulations, we obtain

$$\begin{aligned} \left\{ \frac{(\,r^{[\mathrm{te}]}\,)'}{r^{[\mathrm{te}]}}\,,\, \frac{(\,r^{[\mathrm{tm}]}\,)'}{r^{[\mathrm{tm}]}} \right\} &= 2\,n_1 n_2\,(\,\cos\theta_1\sin\theta_2\,\theta_2' - \sin\theta_1\cos\theta_2\,\theta_1'\,)\ \times \\ &\quad \left\{ \frac{1}{n_1^2\cos^2\theta_1 - n_2^2\cos^2\theta_2}\,,\, \frac{1}{n_2^2\cos^2\theta_1 - n_1^2\cos^2\theta_2} \right\}. \end{aligned} \tag{22}$$

Repeating the procedure for the transmission coefficients, we have

$$\begin{aligned} \left\{ \frac{(\,t^{[\mathrm{te}]}\,)'}{t^{[\mathrm{te}]}}\,,\, \frac{(\,t^{[\mathrm{tm}]}\,)'}{t^{[\mathrm{tm}]}} \right\} &= (\,\cos\theta_1\sin\theta_2\,\theta_2' - \sin\theta_1\cos\theta_2\,\theta_1'\,)\ \times \\ &\quad \left\{ \frac{n_2}{n_1\cos\theta_1 + n_2\cos\theta_2}\,,\, \frac{n_1}{n_2\cos\theta_1 + n_1\cos\theta_2} \right\}. \end{aligned} \tag{23}$$

Noticing that the Snell law, $n_1\sin\theta_1 = n_2\sin\theta_2$, implies

$$n_1\cos\theta_1\,\theta_1' = n_2\cos\theta_2\,\theta_2'\,, \tag{24}$$

and we can rewrite the multiplicative factor that appears in the previous expressions in the following form:

$$\cos\theta_1\sin\theta_2\,\theta_2' - \sin\theta_1\cos\theta_2\,\theta_1' = \frac{n_1^2\cos^2\theta_1 - n_2^2\cos^2\theta_2}{n_1 n_2}\,\tan\theta_2\,\theta_1'\,. \tag{25}$$

Consequently, we arrive at the following reduced expressions for the derivatives of the reflection,

$$\left\{ \frac{(\,r^{[\mathrm{te}]}\,)'}{r^{[\mathrm{te}]}}\,,\, \frac{(\,r^{[\mathrm{tm}]}\,)'}{r^{[\mathrm{tm}]}} \right\} = 2\,\tan\theta_2 \left\{ 1\,,\, \frac{1}{\sin^2\theta_2 - \cos^2\theta_1} \right\} \theta_1'\,, \tag{26}$$

and transmission,

$$\left\{ \frac{(t^{[te]})'}{t^{[te]}}, \frac{(t^{[tm]})'}{t^{[tm]}} \right\} = \left\{ \tan\theta_2 - \tan\theta_1, \frac{\tan\theta_2 - n_1^2 \tan\theta_1 / n_2^2}{\sin^2\theta_2 - \cos^2\theta_1} \right\} \theta_1' , \quad (27)$$

Fresnel coefficients.

Starting from the just-derived derivatives, we can express the Taylor series expansion of the Fresnel coefficients in the case of reflection from the upper interface (where we will have a single Fresnel reflection coefficient), in the case of transmission through the oblique interface (where we will have the product of two Fresnel coefficients—both for transmission), and finally in the case of lateral transmission (where we will have the product of three Fresnel coefficients—two for transmission at the upper and lateral interfaces and one for reflection at the oblique interface).

The beam reflected from the upper interface will be characterized by the following Fresnel coefficient:

$$f_1^{[\sigma]}(\alpha_x) = r_1^{[\sigma]}(\alpha_x) .$$

In the case of the optical prism analyzed in this paper, we have $n_1 = 1$, $\theta_1 = \alpha$, $n_2 = n$, $\theta_2 = \beta$, and $\alpha' = 1$; consequently,

$$f_1^{[\sigma]}(\alpha_x) \approx f_1^{[\sigma]}(\alpha) \left[1 + \rho_1^{[\sigma]}(\alpha) (\alpha_x - \alpha) \right] , \quad (28)$$

where

$$\begin{aligned} &\{ \quad f_1^{[te]}(\alpha) \quad , \quad \rho_1^{[te]}(\alpha) \quad , \quad f_1^{[tm]}(\alpha) \quad , \quad \rho_1^{[tm]}(\alpha) \quad \} = \\ &\{ \quad \frac{\cos\alpha - n\cos\beta}{\cos\alpha + n\cos\beta} \quad , \quad 2\tan\beta \quad , \quad \frac{n\cos\alpha - \cos\beta}{n\cos\alpha + \cos\beta} \quad , \quad \frac{2\tan\beta}{\sin^2\beta - \cos^2\alpha} \quad \} . \end{aligned} \quad (29)$$

The transmission through the oblique interface will be characterized by the product of two transmissions: one through the upper interface and the other through the oblique interface.

$$f_2^{[\sigma]}(\alpha_x) = t_1^{[\sigma]}(\alpha_x)\, t_2^{[\sigma]}(\alpha_x) .$$

Therefore,

$$f_2^{[\sigma]}(\alpha_x) \approx f_2^{[\sigma]}(\alpha) \left[1 + \rho_2^{[\sigma]}(\alpha) (\alpha_x - \alpha) \right] , \quad (30)$$

where

$$\begin{aligned} &\{ \quad f_2^{[te]}(\alpha) \quad , \quad \rho_2^{[te]}(\alpha) \quad \} = \\ &\{ \quad \frac{4n\cos\alpha\cos\beta_*}{(\cos\alpha + n\cos\beta)(n\cos\beta_* + \cos\gamma)} \quad , \quad \tan\beta - \tan\alpha + (\tan\gamma - \tan\beta_*)\beta_*' \quad \} \end{aligned} \quad (31)$$

and

$$\begin{aligned} &\{ \quad f_2^{[tm]}(\alpha) \quad , \quad \rho_2^{[tm]}(\alpha) \quad \} = \\ &\{ \quad \frac{4n\cos\alpha\cos\beta_*}{(n\cos\alpha + \cos\beta)(\cos\beta_* + n\cos\gamma)} \quad , \quad \frac{\tan\beta - \tan\alpha/n^2}{\sin^2\beta - \cos^2\alpha} + \frac{\tan\gamma - n^2\tan\beta_*}{\sin^2\gamma - \cos^2\beta_*}\beta_*' \quad \} . \end{aligned} \quad (32)$$

Observing that $\beta_* = \frac{\pi}{4} + \beta$, we have $\beta_*' = \beta' = \cos\alpha / n\cos\beta$.

Finally, the lateral transmission will be characterized by the product of the transmission through the first upper interface, the reflection from the second oblique interface, and, clearly, the transmission through the third lateral interface, which is shown as follows:

$$f_3^{[\sigma]}(\alpha_x) = t_1^{[\sigma]}(\alpha_x)\, r_2^{[\sigma]}(\alpha_x)\, t_3^{[\sigma]}(\alpha_x)\ .$$

We thus obtain the following series expansion:

$$f_3^{[\sigma]}(\alpha_x) \approx f_3^{[\sigma]}(\alpha)\left[1 + \rho_3^{[\sigma]}(\alpha)\,(\,\alpha_x - \alpha\,)\right], \tag{33}$$

where

$$\begin{aligned}
f_3^{[\mathrm{te}]}(\alpha) &= \frac{4\,n\,\cos\alpha\,\cos\beta}{(\,\cos\alpha + n\,\cos\beta\,)^2}\ \frac{n\,\cos\beta_* - \cos\gamma}{n\,\cos\beta_* + \cos\gamma}\ ,\\
\rho_3^{[\mathrm{te}]}(\alpha) &= \tan\beta - \tan\alpha + (\,2\,\tan\gamma + \tan\alpha - \tan\beta\,)\,\beta'\ ,\\
f_3^{[\mathrm{tm}]}(\alpha) &= \frac{4\,n\,\cos\alpha\,\cos\beta}{(\,n\,\cos\alpha + \cos\beta\,)^2}\ \frac{\cos\beta_* - n\,\cos\gamma}{\cos\beta_* + n\,\cos\gamma}\ ,\\
\rho_3^{[\mathrm{tm}]}(\alpha) &= \frac{\tan\beta - \tan\alpha/n^2}{\sin^2\beta - \cos^2\alpha} + \left(\frac{2\,\tan\gamma}{\sin^2\gamma - \cos^2\beta_*} + \frac{\tan\alpha - n^2\tan\beta}{\sin^2\alpha - \cos^2\beta}\right)\beta'\ .
\end{aligned} \tag{34}$$

At this point, the series expansions obtained allow us to substitute the angular distributions $g_s(\alpha_x, \alpha_y)$ with $f_s^{[\sigma]}(\alpha_x)\, g(\alpha_x, \alpha_y)$ in the integrand function of the electric fields E_s given in Equation (14), thereby yielding

$$\begin{aligned}
E_s^{[\sigma]}(x_s, y, z_s) &= E_0\, f_s^{[\sigma]}(\alpha) \int \mathrm{d}\alpha_x\ \mathrm{d}\alpha_y \left[1 + \rho_s^{[\sigma]}(\alpha)\,(\,\alpha_x - \alpha\,)\right] g(\alpha_x, \alpha_y)\ \times\\
&\quad \exp\left[\, i\,\psi_s(\alpha_x, \alpha_y)\,\right],
\end{aligned} \tag{35}$$

where the optical phase, $\psi_s(\alpha_x, \alpha_y)$, will include not only the spatial component but also the phases of the Fresnel reflection and transmission coefficients. The Fresnel phases will be responsible for determining the optical path predicted by geometric optics. The optical geometric phase, $\psi_s(\alpha_x, \alpha_y)$, will be the focus of the next section's study. The Taylor series expansion of it will lead us to quickly and directly obtain the predicted path of the geometric optics. Equally important, it will provide us with the possibility of analytical integrations for the fields reflected and transmitted by the prism. The new analytical representations will enable us to qualitatively and quantitatively study phenomena such as angular deviations, lateral displacements, and breaks in transverse symmetries more effectively.

4. The Geometrical Phase Analysis

Considering the point where the incident beam intersects the upper face of the prism to be the point of the minimum beam waist, this translates into considering the origin of the axes at this point. In this situation, the optical phase of the reflected beam will not include the Fresnel phase, thus resulting in the following:

$$\psi_1(\alpha_x, \alpha_y)\,/\,k = (\,\widetilde{x}\,\sin\alpha_x - \widetilde{z}\,\cos\alpha_x\,)\,\cos\alpha_y + y\,\sin\alpha_y\ . \tag{36}$$

Expanding up to the second order around the angle $(\alpha_x, \alpha_y) = (\alpha, 0)$

$$\begin{aligned}
\psi_1(\alpha_x, \alpha_y)\,/\,k &\approx \widetilde{x}\,\sin\alpha - \widetilde{z}\,\cos\alpha + (\,\widetilde{x}\,\cos\alpha + \widetilde{z}\,\sin\alpha\,)\,(\,\alpha_x - \alpha\,) + y\,\alpha_y\\
&\quad - (\,\widetilde{x}\,\sin\alpha - \widetilde{z}\,\cos\alpha\,)\,\frac{(\,\alpha_x - \alpha\,)^2 + \alpha_y^2}{2}
\end{aligned} \tag{37}$$

and applying the rotation

$$\begin{pmatrix} x_1 \\ z_1 \end{pmatrix} = \begin{pmatrix} \cos(\pi-\alpha) & -\sin(\pi-\alpha) \\ \sin(\pi-\alpha) & \cos(\pi-\alpha) \end{pmatrix} \begin{pmatrix} \tilde{x} \\ \tilde{z} \end{pmatrix} = \begin{pmatrix} -\cos\alpha & -\sin\alpha \\ \sin\alpha & -\cos\alpha \end{pmatrix} \begin{pmatrix} \tilde{x} \\ \tilde{z} \end{pmatrix}, \tag{38}$$

see Figure 2, we obtain

$$\psi_1(\alpha_x,\alpha_y)\,/\,k \approx z_1 - x_1\,(\,\alpha_x - \alpha\,) + y\,\alpha_y - z\,\frac{(\,\alpha_x-\alpha\,)^2+\alpha_y^2}{2}\,. \tag{39}$$

The integral form of the electric field of the reflected optical beam is then given by

$$E_1^{[\sigma]}(x_1,y,z_1) = E_0\exp[\,i\,k\,z_1\,]\,f_1^{[\sigma]}(\alpha)\int \mathrm{d}\alpha_x\,\mathrm{d}\alpha_y\,\Big[\,1+\rho_1^{[\sigma]}(\alpha)\,(\,\alpha_x-\alpha\,)\Big]\,g(\alpha_x,\alpha_y)\,\times \exp\left\{ i\,k\left[-x_1\,(\,\alpha_x-\alpha\,) + y\,\alpha_y - z_1\,\frac{(\,\alpha_x-\alpha\,)^2+\alpha_y^2}{2}\right]\right\}. \tag{40}$$

Having simplified the integrand that now appears in the expression of the reflected field, we will demonstrate in the next section that we can integrate it to obtain a closed-form formula for the reflected field, which is similar to the one obtained for the incident field. This will allow us to analyze its analytical characteristics and understand which term is responsible for the angular deviations.

Now, let us focus on the phase of the field transmitted through the oblique interface of the optical prism:

$$\psi_2(\alpha_x,\alpha_y)\,/\,k = [\,x_*\,\sin\gamma(\alpha_x) + z_*\,\cos\gamma(\alpha_x)\,]\,\cos\alpha_y + y\,\sin\alpha_y + d_*\,[\,n\,\cos\beta_*(\alpha_x) - \cos\gamma(\alpha_x)\,]\,. \tag{41}$$

In this case, the Fresnel phase, which appears in the expression, will enable us to obtain, when we expand it in a Taylor series, the optical path predicted by the laws of geometric optics. Indeed, the expansion around the angle $(\alpha,0)$ leads to

$$\begin{aligned}\psi_2(\alpha_x,\alpha_y)\,/\,k \approx\ & x_*\,\sin\gamma + z_*\,\cos\gamma + d_*\,(\,n\,\cos\beta_* - \cos\gamma\,) \\ & + \big[\,(\,x_*\,\cos\gamma - z_*\,\sin\gamma\,)\,\gamma' + d_*\,(\,-n\,\sin\beta_*\,\beta_*' + \sin\gamma\,\gamma'\,)\,\big]\,(\,\alpha_x-\alpha\,) \\ & + y\,\alpha_y - (\,x_*\,\sin\gamma + z_*\,\cos\gamma\,)\,\frac{[\,\gamma'\,(\,\alpha_x-\alpha\,)\,]^2+\alpha_y^2}{2}\,.\end{aligned} \tag{42}$$

In the previous expansion, the second-order Taylor series development of the Fresnel phase and the term proportional to the second derivative of gamma have been omitted. This is because only the second-order term presented is proportional to the axial coordinate, as we will soon observe with the rotation that brings us to the proper coordinates of the beam transmitted through the oblique interface. Before rewriting the phase in terms of proper coordinates (x_2,y_2), it is interesting to note that the first-order Taylor expansion immediately allows us to determine the exit point of the beam, as predicted by the geometric optics. Indeed, by considering the exit point as $z_* = d_*$, see Figures 1 and 2, and setting the coefficient multiplying $(\alpha_x-\alpha)$ to zero, we obtain $x_*\,\cos\gamma\,\gamma' = d_*\,n\,\sin\beta_*\,\beta_*'$ and using $\beta_*' = \cos\gamma\,\gamma'\,/\,\cos\beta$, we find

$$x_* = d_*\,\tan\beta_*\,, \tag{43}$$

which is precisely the exit point from the oblique interface, as predicted by geometric optics. Now, by employing the rotation

$$\begin{pmatrix} x_2 \\ z_2 \end{pmatrix} = \begin{pmatrix} \cos\gamma & -\sin\gamma \\ \sin\gamma & \cos\gamma \end{pmatrix} \begin{pmatrix} x_* \\ z_* \end{pmatrix}, \tag{44}$$

see Figure 2, we can rewrite the optical phase (42) in terms of the proper coordinates of the beam:

$$\begin{aligned} \psi_2(\alpha_x,\alpha_y)/k &\approx z_2 + h_2 + (x_2 - d_2)\,\gamma'(\alpha_x - \alpha) + y\,\alpha_y \\ &\quad - z_2\,\frac{[\gamma'(\alpha_x-\alpha)]^2 + \alpha_y^2}{2}, \end{aligned} \tag{45}$$

where

$$d_2 = d_*(n\sin\beta_*\,\beta'_*/\gamma' - \sin\gamma) = d_*(\tan\beta_* - \tan\gamma)\cos\gamma, \tag{46}$$

and it defines the shift from the origin of the proper coordinates of the transmitted beam predicted by the geometric optics. Finally, the integral form of the electric field of the transmitted beam will be given by

$$\begin{aligned} E_2^{[\sigma]}(x_2,y,z_2) &= E_0\exp[\,i\,k\,(z_2+h_2)\,]\,f_2^{[\sigma]}(\alpha)\int d\alpha_x\,d\alpha_y\left[1+\rho_2^{[\sigma]}(\alpha)\,(\alpha_x-\alpha)\right]g(\alpha_x,\alpha_y)\times \\ &\exp\left\{i\,k\left[(x_2-d_2)\,\gamma'(\alpha_x-\alpha) + y\,\alpha_y - z_2\,\frac{[\gamma'(\alpha_x-\alpha)]^2+\alpha_y^2}{2}\right]\right\}. \end{aligned} \tag{47}$$

It is precisely the fact that the term $(\alpha_x - \alpha)$ is multiplied by γ' in the optical phase of the transmitted beam that, as we will see in detail in the next section, will lead, after integration, to the phenomenon of transverse symmetry breaking.

Now, we can proceed to examine the optical phase of the beam transmitted laterally, i.e.,

$$\begin{aligned} \psi_3(\alpha_x,\alpha_y)/k &= (\,\widetilde{z}\sin\alpha_x + \widetilde{x}\cos\alpha_x\,)\cos\alpha_y + y\sin\alpha_y \\ &\quad + 2\,d_*\,n\cos\beta_*(\alpha_x) + (l-d)\,[\,n\cos\beta(\alpha_x) - \cos\alpha_x\,]. \end{aligned} \tag{48}$$

By expanding, as is done for the other optical beams, in a Taylor series around the angle $(\alpha, 0)$, we obtain

$$\begin{aligned} \psi_3(\alpha_x,\alpha_y)/k &\approx (\,\widetilde{z}\sin\alpha + \widetilde{x}\cos\alpha\,) + 2\,d_*\,n\cos\beta_* + (l-d)\,(n\cos\beta - \cos\alpha) \\ &\quad + [\,(\widetilde{z}\cos\alpha - \widetilde{x}\sin\alpha) - 2\,d_*\,n\sin\beta_*\,\beta'_* + \\ &\quad (l-d)\,(-n\sin\beta\,\beta' + \sin\alpha)\,](\alpha_x-\alpha) \\ &\quad + y\,\alpha_y - (\,\widetilde{z}\sin\alpha + \widetilde{x}\cos\alpha\,)\,\frac{(\alpha_x-\alpha)^2+\alpha_y^2}{2}. \end{aligned} \tag{49}$$

As with the beams transmitted through the oblique interface, it is insightful to analyze the coefficients multiplying $\alpha - \alpha_x$ at the exit point of the lateral interface, specifically when $\widetilde{x} = l - d$. By setting this coefficient to zero, we find $\widetilde{z}\cos\alpha = 2\,d_*\,n\sin\beta_*\,\beta'_* + (l-d)\,(n\sin\beta\,\beta')$ and using $\beta'_* = \beta' = \cos\alpha/n\cos\beta$, we obtain

$$\widetilde{z} = d + l\tan\beta, \tag{50}$$

exactly at the point where the oblique interface's exit aligns with the prediction of the geometric optics. Now, employing rotation

$$\begin{pmatrix} x_3 \\ z_3 \end{pmatrix} = \begin{pmatrix} \cos\alpha & -\sin\alpha \\ \sin\alpha & \cos\alpha \end{pmatrix} \begin{pmatrix} \widetilde{z} \\ \widetilde{x} \end{pmatrix}, \tag{51}$$

see Figure 2, we can rewrite the optical phase(49) in terms of the proper coordinates of the beam

$$\psi_3(\alpha_x,\alpha_y)/k \;\approx\; z_3 + h_3 + (x_3 - d_3)(\alpha_x - \alpha) + y\,\alpha_y - z_3\,\frac{(\alpha_x - \alpha)^2 + \alpha_y^2}{2}, \quad (52)$$

where

$$d_3 \;=\; 2\,d_*\,n\,\sin\beta_*\,\beta'_* + (l - d)(n\,\sin\beta\,\beta' - \sin\alpha)\,. \quad (53)$$

The integral form of the electric field of the transmitted beam will be then given by

$$E_3^{[\sigma]}(x_3,y,z_3) \;=\; E_0\exp[\,i\,k\,(z_3 + h_3)\,]\,f_3^{[\sigma]}(\alpha)\int d\alpha_x\,d\alpha_y\left[1 + \rho_3^{[\sigma]}(\alpha)(\alpha_x - \alpha)\right]g(\alpha_x,\alpha_y)\,\times$$
$$\exp\left\{i\,k\left[(x_3 - d_3)(\alpha_x - \alpha) + y\,\alpha_y - z_3\,\frac{[(\alpha_x - \alpha)]^2 + \alpha_y^2}{2}\right]\right\}. \quad (54)$$

We observe that, just as with the reflected beam, in the field transmitted by the lateral interface, the term $\alpha - \alpha_x$and its square are not multiplied by any coefficient. The laterally transmitted beam, like the beam reflected from the upper surface, therefore maintains the transverse symmetry present in the incident beam, unlike what occurs with the beam transmitted by the oblique. The breakdown of transverse symmetry occurs when the transmission angle differs from the incidence angle, as is precisely the case with transmission from the oblique interface.

5. Optical Behavior of the Reflected and Transmitted Beams

In the previous section, we observed how the Taylor series expansion of the optical phase allows us to recover the optical path followed by the beams reflected from the upper interface of the prism, as well as those transmitted through the oblique and lateral interfaces. Extending the Taylor series expansion of the optical phase to the second order, along with the first-order expansion of the Fresnel coefficients conducted in Section 2, also enables us to obtain integrand functions, see Equations (40), (47) and (54), that can now be analytically solved. This provides the opportunity to rewrite the reflected and transmitted beams as functions of the incident electric field given in Equation (13). The ability to represent the reflected and transmitted fields through analytical formulas allows for an immediate understanding of the terms responsible for phenomena such as angular deviations, lateral displacements, and the breakdown of transverse symmetry. Another undeniable advantage is clearly represented by the fact that these analytical formulas can complement any numerical simulations, thereby expediting the computational process in certain technological applications.

5.1. Reflection by the Upper Interface

The integrand function appearing in Equation (40) can be rewritten by substituting the first-order term in the Taylor series expansion of the Fresnel coefficient for the derivative with respect to x_1:

$$E_1^{[\sigma]}(x_1,y,z_1) \;=\; E_0\exp[\,i\,k\,z_1\,]\,f_1^{[\sigma]}(\alpha)\int d\alpha_x\,d\alpha_y\left[1 + \frac{i}{k}\,\rho_1^{[\sigma]}(\alpha)\,\partial_{x_1}\right]g(\alpha_x,\alpha_y)\,\times$$
$$\exp\left\{i\,k\left[-x_1(\alpha_x - \alpha) + y\,\alpha_y - z_1\,\frac{(\alpha_x - \alpha)^2 + \alpha_y^2}{2}\right]\right\}. \quad (55)$$

At this juncture, the beam reflected from the upper interface can be expressed in terms of the incident field (13) as follows:

$$E_1^{[\sigma]}(x_1,y,z_1) = f_1^{[\sigma]}(\alpha)\ \frac{E_0\exp[\,i\,k\,z_1\,]}{1+i\,z_1/z_R}\left[1+\frac{i}{k}\,\rho_1^{[\sigma]}(\alpha)\,\partial_{x_1}\right]\exp\left[-\frac{(\,x_1^2+y^2\,)/w_0^2}{1+i\,z_1/z_R}\right]$$
$$= f_1^{[\sigma]}(\alpha)\ \frac{E_0\exp[\,i\,k\,z_1\,]}{(\,1+i\,z_1/z_R\,)^2}\left[1+i\,\frac{z_1-\rho_1^{[\sigma]}(\alpha)\,x_1}{z_R}\right]\exp\left[-\frac{(\,x_1^2+y^2\,)/w_0^2}{1+i\,z_1/z_R}\right]. \quad (56)$$

Recalling that the terms $f_1^{[\sigma]}(\alpha)$ and $\rho_1^{[\sigma]}(\alpha)$ are real for any angle of incidence, $\sin^2\alpha < n^2$, the intensity of the beam reflected from the upper surface will be given by the following:

$$I_1^{[\sigma]}(x_1,y,z_1) = I_0\left[f_1^{[\sigma]}(\alpha)\right]^2\left[\frac{w_0}{w(z_1)}\right]^4\left\{1+\left[\frac{z_1-\rho_1^{[\sigma]}(\alpha)\,x_1}{z_R}\right]^2\right\}\exp\left[-2\,\frac{x_1^2+y^2}{w^2(z_1)}\right]$$
$$= \left[f_1^{[\sigma]}(\alpha)\right]^2\left[\frac{w_0}{w(z_1)}\right]^2\left\{1+\left[\frac{z_1-\rho_1^{[\sigma]}(\alpha)\,x_1}{z_R}\right]^2\right\}I(x_1,y,z_1) \quad (57)$$
$$\approx \left[f_1^{[\sigma]}(\alpha)\right]^2\left[\frac{w_0}{w(z_1)}\right]^2\left\{\left[\frac{w(z_1)}{w_0}\right]^2-2\,\frac{\rho_1^{[\sigma]}(\alpha)\,x_1\,z_1}{z_R^2}\right\}I(x_1,y,z_1)\,.$$

The approximation made in the reflected beam intensity is justified by the fact that the axial variable is always greater than the transverse variables. For example, when the axial variable is on the order of z_R, the mixed term scales as $1/kw_0$, since the eliminated term scales as $1/(kw_0)^2$. By integrating over transverse coordinates, we obtain the power of the reflected beam, i.e.,

$$P_1^{[\sigma]} = \left[f_1^{[\sigma]}(\alpha)\right]^2 P\,. \quad (58)$$

As expected, the power of the reflected beam equals the incident beam power P, which is modulated by the square of the Fresnel reflection coefficients, which exhibit polarization dependence. Returning to the incident beam, we observe that its spatial distribution is quadratic in the transverse coordinates, x and y, thus implying that the mean values of these coordinates, $\langle x\rangle$ and $\langle y\rangle$, are zero. For the reflected beam, the transverse coordinate y continues to have a zero mean value, but the transverse coordinate x_1 has a mean value given by

$$\langle x_1\rangle_\sigma = \int dx_1\,dy\ x_1\ I_1^{[\sigma]}(x_1,y,z_1)\ /\ P_1^{[\sigma]} = -\,2\,\frac{\rho_1^{[\sigma]}(\alpha)}{(k\,w_0)^2}\ z_1\,. \quad (59)$$

The reflected beam, therefore, deviates from the optical path predicted by the law of reflection, and its deviation is proportional to z_1. From Figure 2, it can be observed that a displacement in the negative direction of the x_1 axis implies a reflection angle greater than that predicted by the law of reflection. Additionally, considering that $k\,w_0 = 2\,\pi\,w_0/\lambda \gg 1$, for an incidence angle α, we will have a reflection angle

$$\alpha_1^{[\sigma]} = \alpha + 2\,\frac{\rho_1^{[\sigma]}(\alpha)}{(k\,w_0)^2}\,. \quad (60)$$

This phenomenon is known as angular deviation and is caused by the symmetry breaking in the angular distribution induced by the modulation performed by the Fresnel reflection coefficients.

5.2. Transmitted by the Oblique Interface

As seen in the previous subsection, a portion of the incident beam will be reflected from the upper interface of the prism, and another portion will be transmitted and will strike the oblique interface, thus forming an angle β_* with the normal. The beam will then be partially transmitted through the oblique interface when $(n\,\sin\beta_*)^2 < 1$. Rewriting this condition in terms of the angle of refraction β, we have

$$-\sin\left[\left(\arcsin\frac{1}{n}+\frac{\pi}{4}\right)\right] \;<\; \sin\beta \;<\; \sin\left(\arcsin\frac{1}{n}-\frac{\pi}{4}\right) \tag{61}$$

And by using $\sin\alpha = n\,\sin\beta$, we can immediately obtain the condition on the angle of incidence α, which ensures that the Fresnel coefficients are real and that the beam is transmitted through the oblique interface, i.e.,

$$-\frac{1+\sqrt{n^2-1}}{\sqrt{2}} \;<\; \sin\alpha \;<\; \frac{1-\sqrt{n^2-1}}{\sqrt{2}}\,. \tag{62}$$

For a refractive index $n = 1.515$, which is the case of a red laser (638 nm) propagating through a BK7 prism, the condition for the transmission at the oblique interface is

$$\alpha \;<\; \alpha_{\rm cri} = -5.603^\circ\,. \tag{63}$$

Note that for angles of incidence greater than the critical angle, the transmitted beam will be characterized by evanescent waves. For an incidence below the critical angle, as was done in the previous subsection, the integrand function appearing in Equation (47) can be rewritten by substituting the first-order term in the Taylor series expansion of the Fresnel coefficient for the derivative with respect to x_2:

$$\begin{aligned}
E_2^{[\sigma]}(x_2,y,z_2) &= E_0\exp[\,i\,k\,(\,z_2+h_2\,)\,]\,f_2^{[\sigma]}(\alpha)\left[1-\frac{i}{k\,\gamma'}\,\rho_2^{[\sigma]}(\alpha)\,\partial_{x_2}\right]\int\!\mathrm{d}\alpha_x\;\mathrm{d}\alpha_y\;\;g(\alpha_x,\alpha_y)\;\times\\
&\qquad \exp\left\{i\,k\left[\,(\,x_2-d_2\,)\,\gamma'\,(\,\alpha_x-\alpha\,)+y\,\alpha_y-z_2\,\frac{[\,\gamma'\,(\,\alpha_x-\alpha\,)\,]^2+\alpha_y^2}{2}\right]\right\}\\
&= E_0\exp[\,i\,k\,(\,z_2+h_2\,)\,]\,f_2^{[\sigma]}(\alpha)\left[1-\frac{i}{k\,\gamma'}\,\rho_2^{[\sigma]}(\alpha)\,\partial_{x_2}\right]\times\\
&\qquad \frac{\exp\left[-\dfrac{(\,x_2-d_2\,)^2\,\gamma'^2/\mathrm{w}_0^2}{1+i\,z_2\,\gamma'^2/z_{\rm R}}\right]}{\sqrt{1+i\,z_2\,\gamma'^2/z_{\rm R}}}\;\frac{\exp\left[-\dfrac{y^2/\mathrm{w}_0^2}{1+i\,z_2/z_{\rm R}}\right]}{\sqrt{1+i\,z_2/z_{\rm R}}}\,.
\end{aligned} \tag{64}$$

Recalling that the terms $f_2^{[\sigma]}(\alpha)$ and $\rho_2^{[\sigma]}(\alpha)$ are real for $\alpha < \alpha_{\rm cri}$, the intensity of the beam transmitted from the oblique surface will be given by the following:

$$\begin{aligned}
I_2^{[\sigma]}(\widetilde{x}_2,y,z_2) &= I_0\left[f_2^{[\sigma]}(\alpha)\right]^2\frac{\mathrm{w}_0}{\mathrm{w}(z_2)}\left[\frac{\widetilde{\mathrm{w}}_0}{\widetilde{\mathrm{w}}(z_2)}\right]^3\left\{1+\left[\frac{z_2+\rho_2^{[\sigma]}(\alpha)\,\widetilde{x}_2/\gamma'}{\widetilde{z}_{\rm R}}\right]^2\right\}\times\\
&\qquad \exp\left[-2\left(\frac{\widetilde{x}_2^2}{\widetilde{\mathrm{w}}^2(z_2)}+\frac{y^2}{\mathrm{w}^2(z_2)}\right)\right]\\
&\approx I_0\left[f_2^{[\sigma]}(\alpha)\right]^2\frac{\mathrm{w}_0}{\mathrm{w}(z_2)}\,\frac{\widetilde{\mathrm{w}}_0}{\widetilde{\mathrm{w}}(z_2)}\left\{1+2\left[\frac{\widetilde{\mathrm{w}}_0}{\widetilde{\mathrm{w}}(z_2)}\right]^2\frac{\rho_2^{[\sigma]}(\alpha)\,\widetilde{x}_2\,z_2}{\gamma'\,\widetilde{z}_{\rm R}^2}\right\}\times\\
&\qquad \exp\left[-2\left(\frac{\widetilde{x}_2^2}{\widetilde{\mathrm{w}}^2(z_2)}+\frac{y^2}{\mathrm{w}^2(z_2)}\right)\right],
\end{aligned} \tag{65}$$

where $\widetilde{x}_2 = x_2 - d_2$, and $\widetilde{w}_0 = w_0 / \gamma'$. By integrating over the transverse coordinates, we obtain the power of the transmitted beam, i.e.,

$$P_2^{[\sigma]} = \left[f_2^{[\sigma]}(\alpha) \right]^2 \frac{\widetilde{w}_0}{w_0} P = \frac{\left[f_2^{[\sigma]}(\alpha) \right]^2}{\gamma'} P . \tag{66}$$

The factor appearing in the denominator is exactly caused by the symmetry breaking between the transverse coordinates and is fundamental for the conservation of intensity. In fact, at this point, we will have the beam reflected from the upper interface, the beam reflected from the oblique interface, and the beam transmitted through the same oblique interface. The conservation of intensity is precisely guaranteed by the presence of the factors in the denominator:

$$\frac{\left[r_1^{[\sigma]}(\alpha) \right]^2}{\alpha'} + \frac{\left[t_1^{[\sigma]}(\alpha)\, r_2^{[\sigma]}(\alpha) \right]^2}{\beta'_*} + \frac{\left[t_1^{[\sigma]}(\alpha)\, t_2^{[\sigma]}(\alpha) \right]^2}{\gamma'} . \tag{67}$$

Indeed, by observing that $\alpha' = 1$, $\cos\gamma\ \gamma' = n \cos\beta_*\ \beta'_*$, and $\beta'_* = \beta' = \cos\alpha / n \cos\beta$, we find

$$\left[r_1^{[\sigma]}(\alpha) \right]^2 + \frac{n \cos\beta}{\cos\alpha} \left[t_1^{[\sigma]}(\alpha) \right]^2 \left\{ \left[r_2^{[\sigma]}(\alpha) \right]^2 + \frac{\cos\gamma}{n \cos\beta_*} \left[t_2^{[\sigma]}(\alpha) \right]^2 \right\} = 1 . \tag{68}$$

As happens with the beam reflected from the upper surface, the beam transmitted through the oblique surface at angles less than the critical angle will also exhibit the phenomenon of angular deviations. The average value of the coordinate $\widetilde{x}_2$ is given by

$$\langle \widetilde{x}_2 \rangle_\sigma = \int \mathrm{d}\widetilde{x}_2\, \mathrm{d}y\ \widetilde{x}_2\, I_2^{[\sigma]}(\widetilde{x}_2, y, z_2) \ / \ P_2^{[\sigma]} = 2\, \frac{\rho_2^{[\sigma]}(\alpha)}{\gamma' \left(k\, \widetilde{w}_0 \right)^2}\ z_2 , \tag{69}$$

which corresponds to an angular deviation compared to the path predicted by geometric optics, which is given by

$$\gamma_2^{[\sigma]} = \gamma + 2\, \frac{\rho_2^{[\sigma]}(\alpha)}{\gamma' \left(k\, \widetilde{w}_0 \right)^2} = \gamma + 2\, \frac{\gamma' \rho_2^{[\sigma]}(\alpha)}{\left(k\, w_0 \right)^2} . \tag{70}$$

We conclude by observing that the breaking of transverse symmetry present in the beam transmitted by the oblique interface, i.e.,

$$\widetilde{w}_0 = \frac{w_0}{\gamma'} = \frac{\cos\beta\, \cos\gamma}{\cos\alpha\, \cos\beta_*}\ w_0 = \mu(\alpha)\ w_0 , \tag{71}$$

allows us to choose incidence angles for which $\widetilde{w}_0$ is greater than w_0 and angles for which it is instead smaller. In the case of a refractive index of 1.515 (BK7 prism and red laser at 638 nm), the angle delimiting the two regions, the solution of $\mu(\alpha) = 1$, is given by -35.434°. The symmetry breaking thus creates two different transverse sections that behave differently, as they propagate in the axial direction z_2. The smaller section will tend to increase more rapidly than the larger one, and therefore, we will always have an axial position where symmetry is restored. This axial coordinate is given by the following:

$$z_2 = \mu(\alpha)\ z_R . \tag{72}$$

5.3. Transmission by the Lateral Interface

As has been done for the reflected beam at the upper interface and for the beam transmitted by the oblique interface, it is convenient to write the field of the beam transmitted by the lateral interface using the derivative of the transverse coordinate x_3 as follows:

$$
\begin{aligned}
E_3^{[\sigma]}(x_3,y,z_3) &= E_0 \exp[\,i\,k\,(\,z_3\,+\,h_3\,)\,]\,f_3^{[\sigma]}(\alpha)\left[\,1\,-\,\frac{i}{k}\,\rho_3^{[\sigma]}(\alpha)\,\partial_{x_3}\right]\int \mathrm{d}\alpha_x\;\mathrm{d}\alpha_y\;\; g(\alpha_x,\alpha_y)\;\times \\
&\quad \exp\left\{\,i\,k\left[\,(\,x_3\,-\,d_3\,)\,(\,\alpha_x-\alpha\,)\,+\,y\,\alpha_y\,-\,z_3\,\frac{[\,(\,\alpha_x-\alpha\,)\,]^2\,+\,\alpha_y^2}{2}\right]\right\} \\
&= E_0 \exp[\,i\,k\,(\,z_3\,+\,h_3\,)\,]\,f_3^{[\sigma]}(\alpha)\left[\,1\,-\,\frac{i}{k}\,\rho_3^{[\sigma]}(\alpha)\,\partial_{x_3}\right]\times \\
&\quad \exp\left[\,-\,\frac{(\,x_3\,-\,d_3)^2\,+\,y^2}{\mathrm{w}_0^2\,(\,1\,+\,i\,z_3\,/\,z_\mathrm{R}\,)}\right]\,/\,(\,1\,+\,i\,z_3\,/\,z_\mathrm{R}\,)\;.
\end{aligned}
\tag{73}
$$

As a first observation, we note that for the beam transmitted through the lateral surface, unlike what happens for the beam transmitted through the oblique surface, we do not have a breaking of transverse symmetry. This is due to the fact that the transmission angle at this interface is equal to the angle of incidence α. A second important difference is that we will have a nonevanescent transmitted beam not only for angles of incidence lower than the critical angle (as is the case for the beam transmitted through the oblique interface) but also for higher angles. Mathematically, this will result in having both the real and imaginary parts of $\rho_3^{[\sigma]}(\alpha)$ in the intensity of the field transmitted, i.e.,

$$
\begin{aligned}
I_3^{[\sigma]}(\widetilde{x}_3,y,z_3) &= I_0\left[\,f_3^{[\sigma]}(\alpha)\,\right]^2\left[\frac{\mathrm{w}_0}{\mathrm{w}(z_3)}\right]^4\times \\
&\quad \left\{\left[\,1\,-\,\frac{\mathrm{Im}[\rho_3^{[\sigma]}(\alpha)]\,\widetilde{x}_3}{z_\mathrm{R}}\right]^2+\left[\frac{z_3\,+\,\mathrm{Re}[\rho_3^{[\sigma]}(\alpha)]\,\widetilde{x}_3}{z_\mathrm{R}}\right]^2\right\}\,\exp\left[\,-2\,\frac{\widetilde{x}_3^2\,+\,y^2}{\mathrm{w}^2(z_3)}\right] \\
&\approx \left[\,f_3^{[\sigma]}(\alpha)\,\right]^2\left[\frac{\mathrm{w}_0}{\mathrm{w}(z_3)}\right]^2\left\{\left[\frac{\mathrm{w}(z_3)}{\mathrm{w}_0}\right]^2\,-\,2\,\frac{\mathrm{Im}[\rho_3^{[\sigma]}(\alpha)]\,\widetilde{x}_3}{z_\mathrm{R}}\,+\,2\,\frac{\mathrm{Re}[\rho_3^{[\sigma]}(\alpha)]\,\widetilde{x}_3\,z_3}{z_\mathrm{R}^2}\right\}\times \\
&\quad I(\widetilde{x}_3,y,z_3)\;,
\end{aligned}
\tag{74}
$$

where $\widetilde{x}_3 = x_3\,-\,d_3$, and in the last approximation, we have considered only the first-order terms in $\widetilde{x}_3\,/\,z_\mathrm{R}$. The power of the beam transmitted by the lateral interface is therefore given by

$$
P_3^{[\sigma]} \;=\; \left[\,f_3^{[\sigma]}(\alpha)\,\right]^2\,P\;, \tag{75}
$$

and the average value of the transverse coordinate $\widetilde{x}_3$ is

$$
\begin{aligned}
\langle\widetilde{x}_3\rangle_\sigma &= \int \mathrm{d}\widetilde{x}_3\,\mathrm{d}y\;\;\widetilde{x}_3\;I_3^{[\sigma]}(\widetilde{x}_3,y,z_1)\;/\;P_3^{[\sigma]} \\
&= 2\,\frac{\mathrm{Re}[\rho_3^{[\sigma]}(\alpha)]}{(k\,\mathrm{w}_0)^2}\;\;z_3\,-\,\frac{\lambda}{2\,\pi}\,\mathrm{Im}[\rho_3^{[\sigma]}(\alpha)]\;.
\end{aligned}
\tag{76}
$$

For angles of incidence lower than the critical angle, $\rho_3^{[\sigma]}(\alpha)$ is real, and we observe the phenomenon of angular deviations, i.e.,

$$
\alpha_3^{[\sigma]}(\alpha<\alpha_\mathrm{cri}) \;=\; \alpha\,+\,2\,\frac{\rho_3^{[\sigma]}(\alpha)}{(k\,\mathrm{w}_0)^2}\;. \tag{77}
$$

For angles of incidence greater than the critical angle, $\rho_3^{[\sigma]}(\alpha)$ is complex, and in addition to the phenomenon of angular deviations,

$$\alpha_3^{[\sigma]}(\alpha > \alpha_{\text{cri}}) \;=\; \alpha + 2\,\frac{\text{Re}[\rho_3^{[\sigma]}(\alpha)]}{(k\,\text{w}_0)^2}\;. \tag{78}$$

A lateral displacement appears,

$$s_3^{[\sigma]}(\alpha > \alpha_{\text{cri}}) \;=\; -\frac{\lambda}{2\,\pi}\,\text{Im}[\rho_3^{[\sigma]}(\alpha)]\;, \tag{79}$$

which is the displacement known as the Goos–Hänchen shift [16,18]. For the beam transmitted laterally in the case of an incidence greater than the critical angle, angular deviations and lateral displacements are effects that must be considered simultaneously and can compensate each other. This occurs at the axial distance given by

$$z_3 \;=\; \frac{\text{Im}[\rho_3^{[\sigma]}(\alpha)]}{\text{Re}[\rho_3^{[\sigma]}(\alpha)]}\;z_{\text{R}}\;. \tag{80}$$

6. Discussions

The importance of having an analytical tutorial for the qualitative and quantitative discussion of optical phenomena cannot be overstated. Such a tutorial is crucial for understanding complex behaviors like angular deviations caused by symmetry breaking in the angular distribution due to the angular dependence of Fresnel coefficients. It also provides insights into lateral shifts resulting from additional phase factors in the Fresnel coefficients during total internal reflection. Moreover, the tutorial elucidates the breaking of symmetry in coordinates transverse to the axial direction, which is caused by the difference between the angles of incidence and transmission.

By offering a detailed analytical framework, the tutorial equips readers with a comprehensive understanding of these phenomena. It helps clarify how the Fresnel coefficients influence the angular distribution, thus leading to deviations from the expected optical paths. Furthermore, it explains the Goos–Hänchen effect, where the lateral shift occurs due to phase variations, and it highlights the conditions under which transverse symmetry breaking takes place. This approach not only enhances the theoretical comprehension but also aids in practical applications, thereby making it an invaluable resource for anyone studying or working with optical systems.

The possibility of obtaining analytical expressions for a laser beam reflected and transmitted by an optical prism helps to understand the cause of phenomena such as angular deviations, lateral displacements, and the breaking of transverse symmetry.

Angular deviations are caused by the fact that the angular distribution of the incident beam, being Gaussian, is a symmetric distribution modulated by the Fresnel coefficients, which thus break this angular symmetry. Angular deviation is seen by calculating the mean value of the transverse coordinate in the plane of incidence of the optical beam, and this can be done analytically once the Fresnel coefficient is developed into a Taylor series. The phenomenon of pure angular deviations occurs for the reflected beam at any angle of incidence, while for transmitted beams, it occurs when the angle of incidence is less than the critical angle,

$$\{\,\alpha_1^{[\sigma]}(\alpha)\,,\,\gamma_2^{[\sigma]}(\alpha < \alpha_{\text{cri}})\,,\,\alpha_3^{[\sigma]}(\alpha < \alpha_{\text{cri}})\,\} \;=\; \{\,\alpha\,,\,\gamma\,,\,\alpha\,\} \;+\; \frac{2}{(k\,\text{w}_0)^2}\,\{\,\rho_1^{[\sigma]}\,,\,\gamma'\,\rho_2^{[\sigma]}\,,\,\rho_3^{[\sigma]}\,\}\;.$$

From the derived analytical formulas, it is observed that for the reflected beam and the beams transmitted through the oblique and lateral interfaces, the angular deviations are proportional to $(\,\lambda\,/\text{w}_0\,)^2$. This means that for a red laser (638 nm) with a beam waist of 100 microns, the angular deviations will be on the order of 0.4×10^{-4} radians.

For the beam transmitted laterally and for angles of incidence greater than the critical angle, the phenomenon of angular deviations is always accompanied by the lateral displacement of Goos–Hänchen,

$$\{\, \alpha_3^{[\sigma]}(\alpha > \alpha_{\text{cri}})\,,\, s_3^{[\sigma]}(\alpha > \alpha_{\text{cri}})\,\} \;\; = \;\; \left\{ \alpha + 2\,\frac{\text{Re}[\rho_3^{[\sigma]}]}{(k\,\text{w}_0)^2}\,,\, -\frac{\lambda}{2\,\pi}\,\text{Im}[\rho_3^{[\sigma]}] \right\}.$$

For angles of incidence near the critical angle, $\gamma = \gamma_{\text{cri}} \pm \delta\,/\,k\,\text{w}_0$, we have $\cos\gamma \approx \mp\,\delta\,/\,k\,\text{w}_0$. Therefore, observing that $\tan\gamma$ and γ' will be proportional to $k\,\text{w}_0$, we will have, for incidences close to the critical incidence, an amplification of the angular deviations and lateral displacement given by $k\,\text{w}_0$. The angular deviations will therefore be proportional to $\lambda\,/\,\text{w}_0$, thus resulting in angular deviations on the order of 0.6×10^{-2} radians. The Goos–Hänchen lateral displacement will change from λ (638 nm) to w_0 (100 microns), thus facilitating its experimental detection.

In the analytical review of the transmitted beams, we also had the opportunity to obtain formulas for the axial coordinate z_2, for which the breaking of transverse symmetry in the case of the field transmitted by the oblique interface is recovered, and for the axial coordinate z_3, for which the effects of angular deviations and lateral displacements compensate each other, i.e.,

$$\{\, z_2(\alpha < \alpha_{\text{cri}})\,,\, z_3(\alpha > \alpha_{\text{cri}})\,\} \;\; = \;\; \left\{ \mu\,,\, \frac{\text{Im}[\rho_3^{[\sigma]}(\alpha)]}{\text{Re}[\rho_3^{[\sigma]}(\alpha)]} \right\} z_{\text{R}}\,. \tag{81}$$

Finally, the ability to have analytical formulas for the fields reflected and transmitted by an optical prism not only offers the clear advantage of avoiding numerical calculations to quantify effects such as angular deviations, lateral displacements, and transverse symmetry breaking, thereby expediting theoretical simulation in preparation for experiments or potential technological applications, but it also enables an understanding of which parameters need to be studied and analyzed to amplify the effects under investigation. For example, one of the well-known amplification techniques in optics is that of weak measurement [9,26], which bases its calculation on the interference between electric and magnetic transverse waves. These waves, exhibiting different behaviors for angular deviations and lateral displacements, result in a nonzero interference that amplifies both the angular deviations and lateral displacements. For such a technique, it is of fundamental importance to have analytical formulas for the electric fields, and therefore, the formulas obtained in this article can be immediately used to implement weak measurement in experimental setups.

The analytical techniques proposed in this tutorial can be effectively applied to the case of a resonant plasmonic surface (dielectric/metal/air) by incorporating the imaginary part of the refractive index that characterizes the metal in the plasmonic structure [28]. By integrating the imaginary component into the Fresnel coefficients and other relevant equations, the tutorial enables quantitative predictions of phenomena like angular deviations and lateral shifts in the context of plasmonic systems. These predictions are essential for optimizing device performance, understanding light confinement effects, and designing applications such as sensors, photodetectors, and nanoscale optical elements. In summary, the analytical techniques provide a powerful framework for studying and manipulating plasmonic resonances, thus offering insights into how these structures interact with light and paving the way for advanced applications in optics and photonics.

Author Contributions: Conceptualization, S.D.L. and M.M.; methodology, S.D.L. and M.M.; software, S.D.L.; validation, S.D.L. and M.M.; formal analysis, S.D.L.; investigation, S.D.L. and M.M.; writing, S.D.L.; review and editing, S.D.L. and M.M.; visualization, S.D.L. and M.M. All authors have read and agreed to the published version of the manuscript.

Funding: This research was funded by the CNPq (Conselho Nacional de Desenvolvimento Científico e Tecnológico) in Brazil, with Grant ID 307664/2021-0 (S.D.L.).

Informed Consent Statement: Not applicable.

Data Availability Statement: All data generated or analyzed during this study are included in this published article.

Acknowledgments: The authors thank an anonymous referee for suggesting the possibility of extending the study to the case of resonant plasmonic surfaces.

Conflicts of Interest: The authors declare no conflicts of interest.

References

1. Born, A.M.; Wolf, E. *Principles of Optics*; Cambridge University Press: Cambridge, UK, 1999.
2. Saleh, B.E.A.; Teich, M.C. *Fundamental of Photonics*; Wiley & Sons: Hoboken, NJ, USA, 2007.
3. Svelto, O. *Principles of Lasers*; Springer: Berlin/Heidelberg, Germany, 2010.
4. Keiser, G. *Optical Fiber Communications*; McGraw-Hill Education: New York, NY, USA, 2019.
5. Ellerbroek, B.L. *Laser Guide Star Adaptive Optics for Astronomy*; Springer: Berlin/Heidelberg, Germany, 2007.
6. Birngruber, R.; Steiner, H. *Lasers in Medicine*; Springer: Berlin/Heidelberg, Germany, 2011.
7. White, I.A.; Snyder, A.W.; Pask, C. Directional change of beams undergoing partial reflection. *J. Opt. Soc. Am.* **1977**, *67*, 703–705. [CrossRef]
8. Chan, C.C.; Tamir, T. Angular shift of a Gaussian beam reflected near the Brewster angle. *Opt. Lett.* **1985**, *10*, 378–380. [CrossRef] [PubMed]
9. Merano, M.; Aiello, A.; van Exter, M.P.; Woerdman, J.P. Observing angular deviations in the specular reflection of a light beam. *Nat. Photonics* **2009**, *3*, 337–340. [CrossRef]
10. Araujo, M.; De Leo, S.; Maia, G. Optimizing weak measurements to detect angular deviations. *Ann. Phys.* **2017**, *529*, 1600357. [CrossRef]
11. Horowitz, B.R.; Tamir, T. Lateral displacement of a light beam at a dielectric interface. *J. Opt. Soc. Am.* **1970**, *61*, 586–594. [CrossRef]
12. Soboleva, I.V.; Moskalenko, V.V.; Fedyanin, A.A. Giant Goos-Hänchen effect and Fano resonance at photonic crystal surfaces. *Phys. Rev. Lett.* **2012**, *108*, 123901. [CrossRef] [PubMed]
13. Bliokh, K.Y.; Aiello, A. Goos–Hänchen and Imbert–Fedorov beam shifts: An overview. *J. Opt.* **2013**, *15*, 014001. [CrossRef]
14. Araujo, M.; De Leo, S.; Maia, G. Oscillatory behavior of light in the composite Goos-Hänchen shift. *Phys. Rev. A* **2017**, *95*, 053836. [CrossRef]
15. Othman, A.; Asiri, S.; Al-Amri, M. Controllable large positive and negative Goos–Hänchen shifts with a double-Lambda atomic system. *Sci. Rep.* **2023**, *13*, 3789. [CrossRef]
16. Goos, F.; Hänchen, H. Ein Neuer Und Fundamentaler Versuch Zur Totalreflexion. *Ann. Phys.* **1947**, *436*, 333–346.
17. Artmann, K. BerechnungDer SeitenversetzungDes Totalreflektierten Strahles. *Ann. Phys.* **1948**, *437*, 87–102. [CrossRef]
18. Goos, F.; Hänchen, H. Neumessung Des Strahlwersetzungseffektes Bei Totalreflexion. *Ann. Phys.* **1949**, *440*, 251–252. [CrossRef]
19. Merano, M.; Aiello, A.; Hooft, G.W.M.; van Exter, P.; Eliel, E.R.; Woerdman, J.P. Observation of Goos-Hänchen shifts in metallic reflection. *Opt. Lett.* **2007**, *15*, 15928–15934. [CrossRef] [PubMed]
20. Santana, O.; Carvalho, S.; De Leo, S.; de Araujo, L. Weak measurement of the composite Goos-Haenchen shift in the critical region. *Opt. Lett.* **2016**, *41*, 3884–3887. [CrossRef] [PubMed]
21. Zhu, G.; Gao, B.; Zhang, J.; Wang, L.G. Experimental proof on the effect of beam width and spatial coherence on Goos-Hänchen shift. *Opt. Laser Technol.* **2023**, *159*, 109027. [CrossRef]
22. Cohen-Tannoudji, C.; Diu, B.; Laloe, F. *Quantum Mechanics*; Wiley: Hoboken, NJ, USA, 2020.
23. Hauge, E.H.; Stovneng, J.A. Tunneling times: A critical review. *Rev. Mod. Phys.* **1989**, *61*, 917–936. [CrossRef]
24. Platero, G.; Aguado, R. Photon-assisted transport in semiconductor nanostructures. *Phys. Rep.* **2004**, *395*, 1–157. [CrossRef]
25. Boev, M.V.; Kovalev, V.M.; Kibis, O.V. Optically induced resonant tunneling of electrons in nanostructures. *Sci. Rep.* **2023**, *13*, 19625. [CrossRef]
26. Jayaswal, G.; Mistura, G.; Merano, M. Observing angular deviations in light-beam reflection via weak measurements. *Opt. Exp.* **2014**, *39*, 6257–6260.
27. De Leo, S. Laser planar trapping. *Laser Phys. Lett.* **2020**, *17*, 116001. [CrossRef]
28. Petrov, N.I.; Danilov, V.A.; Popov, V.V.; Usievich, B.A. Large positive and negative Goos-Hänchen shifts near the surface plasmon resonance in subwavelength grating. *Opt. Exp.* **2020**, *28*, 7552–7564. [CrossRef] [PubMed]